Photochemistry and Photobiology, 2000, 72(2): 163–171

Photodecarboxylation of Ketoprofen in Aqueous Solution. A Time-resolved Laser-induced Optoacoustic Study¶

Claudio D. Borsarelli*[1], Silvia E. Braslavsky[2], Salvatore Sortino[3,4], Giancarlo Marconi[3] and Sandra Monti[3]

[1]Departamento de Química y Física, Universidad Nacional de Rio Cuarto, Rio Cuarto, Argentina;
[2]Max-Planck-Institut für Strahlenchemie, Mülheim an der Ruhr, Germany;
[3]Istituto di Fotochimica e Radiazioni d' Alta Energia del CNR, Area della Ricerca, Bologna, Italy and
[4]Dipartimento di Scienze Chimiche, Università di Catania, Catania, Italy

Received 15 February 2000; accepted 3 May 2000

ABSTRACT

The photodecarboxylation reaction of 2-(3-benzoylphenyl)propionate (ketoprofen anion, KP^-) was studied in water and in 0.1 *M* phosphate buffer solutions in the pH range 5.7–11.0 by laser-induced optoacoustic spectroscopy (LIOAS, *T* range 9.5–31.6°C). Upon exciting KP^- with 355 nm laser pulses under anaerobic conditions, two components in the LIOAS signals with well-separated lifetimes were found ($\tau_1 < 20$ ns; $250 < \tau_2 < 500$ ns) in the whole pH range, whereas a long-lived third component ($4 < \tau_3 < 10$ μs) was only detected at pH ≤ 6.1. The heat and structural volume changes accompanying the first step did not depend on pH or on the presence of buffer. The carbanion resulting from prompt decarboxylation within the nanosecond pulse (<10 ns) drastically reduces its molar volume ([−18.9 ± 2.0] cm^3/mol) with respect to KP^- and its enthalpy content is (256 ± 10) kJ/mol. At acid pH (*ca* 6), a species is formed with a lifetime in the hundreds of ns. The enthalpy and structural volume change for this species with respect to KP^- are (181 ± 15) kJ/mol and (+0.6 ± 2.0) cm^3/mol, respectively. This species is most likely a neutral biradical formed by protonation of the decarboxylated carbanion, and decays to the final product 3-ethylbenzophenone in several μs. At basic pH (*ca* 11), direct formation of 3-ethylbenzophenone occurs in hundreds of ns involving a reaction with the solvent. The global decarboxylation reaction is endothermic ([45 ± 15] kJ/mol) and shows an expansion of (+14.5 ± 0.5) cm^3/mol with respect to KP^-. At low pH, the presence of buffer strongly affects the magnitude of the structural volume changes associated with the intermolecular proton-transfer processes of the long-lived species due to reactions of the buffer anion with the decarboxylated ketoprofen anion.

INTRODUCTION

Photodecarboxylation processes play an important role in many photochemical reactions (1), especially with drugs containing the benzophenone chromophore (2), such as the 2-(3-benzoylphenyl)propionic acid (ketoprofen, KPH†). This compound is a nonsteroidal antiinflammatory drug frequently used in the treatment of rheumatic diseases by topical application. In view of the possibility of direct exposure of the applied drug to sunlight and considering that its chemical structure is that of a substituted benzophenone, it is important to characterize its photochemical behavior. It has been shown that KPH acts as photosensitizer for biological substrates producing toxic effects, such as lipid peroxidation and DNA cleavage, both *in vivo* and *in vitro* (3–6).

Exposure of KPH in neutral aqueous solutions to sunlight or UV light results in a rapid consumption of the drug. Product studies of the steady-state photolysis of KPH have shown an efficient CO_2 loss (photodecarboxylation quantum yield of 0.75) that only occurs from the deprotonated form of the drug (KP^-, $pK_a = 4.7$) (3,7). Under anaerobic conditions KP^- is only converted to 3-ethylbenzophenone, whereas in the presence of oxygen several photoproducts are formed in addition to 3-ethylbenzophenone, and the product distribution is influenced by the initial KPH concentration and the irradiation time (3,7).

Two laser-flash photolysis studies have been performed in order to characterize the nature of the transient species produced upon excitation of KPH in aqueous solutions (8,9). Monti *et al.* (8) used both ps and ns laser excitation at 266 and 355 nm. They monitored at pH 7.4 the ''prompt'' formation of the triplet state of KP^- ($\lambda_{max} = 526$ nm) followed by a fast decay (250 ps lifetime) to a transient intermediate with a 570 nm absorption maximum and a decay lifetime of *ca* 120 ns. This latter intermediate was proposed to be a triplet biradical anion, formed by intramolecular electron transfer from the carboxyl to the carbonyl group, decarboxylating adiabatically on the nanosecond time scale. The authors also detected longer-lived transient species (with lifetimes ≥4 μs) with absorption maxima at 330 and 520 nm.

¶Posted on the web on 24 May 2000.

*To whom correspondence should be addressed at: Departamento de Ciencias Básicas, Facultad de Agronomía y Agroindustrias, Universidad de Santiago del Estero, Av. Belgrano (5) 1912, Santiago del Estero, 4200 Argentina.
e-mail: cborsarelli@exa.unrc.edu.ar

†*Abbreviations:* KPH, ketoprofen; KP^-, ketoprofen carboxylate anion; LIOAS, laser-induced optoacoustic spectroscopy; MM+, Molecular Mechanics method.

The absorbance changes at both wavelengths were pH dependent, and a protonation equilibrium, involving a neutral biradical and showing a pK_a *ca* 7.6 was suggested.

Martínez and Scaiano (9) suggested a ''prompt'' decarboxylation step followed by ''slow'' protonation by the solvent (the rate of this process was shown to be pH-dependent). The transient intermediate formed after CO_2 loss displayed spectroscopic features reminiscent of a ketyl radical anion and a benzylic radical, and its absorption maxima were at 330 and 600 nm (9). It was also proposed that the photodegradation of KP^- in aqueous solutions occurs mainly through an ionic mechanism involving either the singlet excited state or a very short-lived triplet state.

Regarding the decarboxylation step, the suggested mechanisms differ in the time domain where the process takes place. Recently, from the analysis of the Arrhenius parameters of the decay of the transient with a lifetime of *ca* 200 ns at room temperature in organic solvent–water mixtures, it was concluded that this species could not suffer decarboxylation. Rather, fast decarboxylation should take place within the 8 ns laser pulse (10). It was also concluded that the precursor of the carbanion absorbing in the visible should be the singlet excited state of KP^- instead of a short-lived triplet state (10).

In order to contribute to the understanding of the time course of the decarboxylation reaction, we decided to investigate the dynamics of CO_2 loss from KP^- by employing time-resolved laser-induced optoacoustic spectroscopy (LIOAS). LIOAS allows the simultaneous determination of the time-resolved structural volume changes and enthalpy changes after laser excitation in a time range of few ns to several μs.

We support a ''prompt'' decarboxylation of KP^- in aqueous solutions under anaerobic conditions and a pH-dependent mechanism for the formation of the final product. Furthermore, the enthalpy content and the structural volume changes of the transient species and stable product of the reaction are reported.

EXPERIMENTAL

Materials. KPH and Evans blue (Sigma) were used as received. HCl, NaOH, NaH_2PO_4 and Na_2HPO_4 were Merck p.a. degree. Water was triply distilled.

Methods. The LIOAS experiments were performed in Rio Cuarto (Argentina) and in Mülheim an der Ruhr (Germany) by using in both cases a very similar experimental setup. The excitation sources were a 20 ns (Rio Cuarto) and a 10 ns (Mülheim), 355 nm laser pulse produced by an Nd:YAG laser (Spectron SL400 and SL456G, respectively) operating at 1 Hz. The laser beam width was shaped with a rectangular slit (0.5 width × 5 height) mm, which allows a time resolution during the LIOAS experiments from *ca* 20 ns up to <10 μs using deconvolution techniques. The total laser energy after the slit was <40 μJ per pulse, measured with a pyroelectric energy meter Melles-Griot model 13PEM001 (Rio Cuarto) and Laser Precision Corp. RJP735 head connected to a meter model RJ7620 (Mülheim). The pressure wave was detected with a ceramic piezoelectric transducer spring-loaded to the cuvette window parallel to the laser beam direction. The signals were amplified 100 times (2× Comlinear E103) and fed into a transient recorder Hewlett–Packard 54504 (Rio Cuarto) and Tektronik TDS 684A (Mülheim). In order to avoid sample consumption no more than 10 signals were averaged.

Typically, the samples were prepared by stirring KPH in 1×10^{-4} *M* NaOH aqueous solutions in the dark and under N_2 atmosphere during 4–6 h. KPH was added until saturation. Afterwards, the solutions were filtered in order to avoid light-scattering effects by solid particles. The pH value of these solutions was *ca* 5.5. The final pH was adjusted (±0.1 units) to the desired values (pH 6.1, 7.5 and 10.9) with NaOH-concentrated solutions under N_2 atmosphere, in order to remove residual CO_2. Similar procedure was performed for the sample preparation in 0.1 *M* phosphate buffer solutions, at pH 5.7, 7.4 and 11.0 (±0.1 units) adjusted with concentrated HCl or NaOH solutions.

In all cases, the absorbance of the samples at 355 nm was *ca* 0.1 as recorded with a Shimadzu UV-2102PC spectrophotometer. Under these conditions, the concentration of KPH was estimated at *ca* 1 m*M*. An Evans blue solution at the respective pH values was matched in absorbance (±3%) at 355 nm with that of the sample, and used as calorimetric reference. In all cases, the solutions were degassed by bubbling with water-saturated argon for 15–20 min. The temperature range for the LIOAS experiments was 9.5–31.6 (±0.1)°C. The pH values of the solutions were monitored before and after each experiment, and in all cases they were unchanged.

The signal function *S(t)* in LIOAS is the convolution of the instrumental function *R(t)* (the signal of the calorimetric reference) and the sample function *H(t)* (Eq. 1) (11),

$$S(t) = R(t) \otimes H(t) \tag{1}$$

with

$$H(t) = \sum_i \frac{\varphi_i}{\tau_i} \exp\left(-\frac{t}{\tau_i}\right) \tag{2}$$

where φ_i and τ_i are the amplitude factor and lifetime for the *i*th transient, respectively (11). The signals were analyzed by a deconvolution procedure using a multiexponential sequential kinetic model supplied by the Sound Analysis 3000 1.13 software (Quantum Northwest Inc.).

A geometrical optimization of ground state KP^- and of the various intermediates hypothesized during the photodecarboxylation process was performed using the Molecular Mechanics method (MM+). The energies, heats of formation and dipole moments were calculated using the ZINDO/1 method, as indicated in the Hyperchem 3.1 software package (Hypercube Inc.). The solvent accessible surfaces were calculated by means of the program MSEED (12).

The structural volume changes occurring during the deactivation steps were calculated using standard equations based on the solvent continuum model that take into account the variation of dipole moments and molecular size of the solute in a given solvent (13,14), and neglecting in a first approximation possible specific solute–solvent interactions playing a fundamental role in aqueous solutions (15,16).

RESULTS

LIOAS measurements in water solutions

Under our pH conditions KPH is present as carboxylate anion, KP^-, because its $pK_a = 4.7$ (3,7). Therefore, in the following text we will refer only to this species. In all cases the plots of the LIOAS signal amplitude for KP^- *vs* the laser total energy were linear with zero intercepts within the total energy range studied (<40 μJ per pulse). This indicates that biphotonic processes or signal saturation do not take place.

Figure 1 shows typical LIOAS signals after laser excitation of KP^- at pH 6.1 and 10.9, together with the signal of the calorimetric reference Evans blue under the same conditions.

Taking into account that the photochemistry of KP^- at pH > 4.7 involves the formation of transient species with lifetimes ranging from ps to μs (8–10), we applied the deconvolution technique (see ''Experimental'') in order to separate the contributions of the transients species to the LIOAS signal. Satisfactory fits were obtained with a sum of three exponential decays in the fitting function at pH 6.1, and with a sum of two exponential decays in the fitting function at

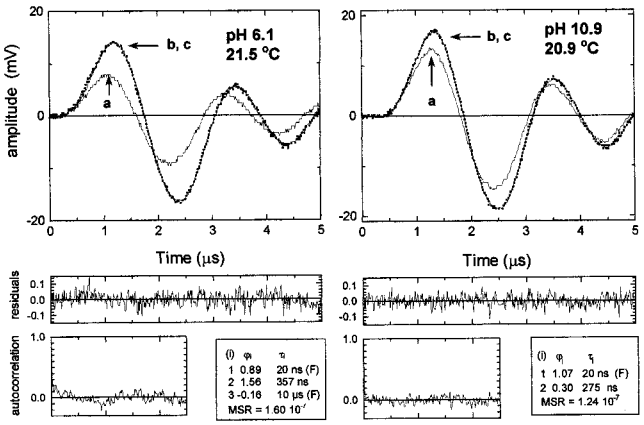

Figure 1. LIOAS signals for Evans blue (curve a) and KP^- (curve b) in water at pH 6.1 and 10.9, together with the fit (curve c), residuals distribution and autocorrelation waveforms after the deconvolution procedure. Laser total energy = 30 μJ per pulse. λ_{exc} = 355 nm.

other pH values (see Fig. 1). In all cases, the program found well-separated lifetimes: $\tau_1 < 20$ ns, $200 < \tau_2 < 550$ ns (depending on pH and temperature), and $\tau_3 > 4$ μs only at pH 6.1. These lifetimes were associated with sequential reaction steps (*vide infra*).

The value of $\tau_1 < 20$ ns only means that the related process is faster than the time resolution of our experimental setup (*ca* 20 ns in the Rio Cuarto system). In fact, fixing this parameter at any value between 0.1 and 20 ns always resulted in the same value of the preexponential factor φ_1. Therefore, φ_1 is a reliable measure of all ''prompt'' processes. Instead, the lifetime of the second component, τ_2, was found to be pH and temperature dependent (Table 1). The range of τ_2 at room temperature is in agreement with the lifetime of the visible-absorbing transient species formed after excitation of KP^- and characterized by laser-flash photolysis under similar conditions as those used in the present study (8–10). At pH 6.1, the third decay time τ_3 was far too long and close to our upper detection limit of the LIOAS method (*ca* < 10 μs), and then the associated amplitude factor φ_3 may be affected by slight differences in baseline between sample and reference signals. Therefore, τ_3 was fixed at a long decay of 10 μs; otherwise the program would calculate interpolated values for the other lifetimes and amplitudes.

The temperature dependence of τ_2 follows an Arrhenius behavior (Fig. 2) with activation energies of (24 ± 1), (19 ± 1) and (18 ± 1) kJ/mol and preexponential factors of 5.3×10^{10}, 7.2×10^9 and 5.9×10^9 s^{-1} at pH 6.1, 7.5 and 10.9, respectively.

In LIOAS, the separation of the thermal and the structural volume change contribution to the acoustic wave for each transient species formed after laser excitation is based on (Eq. 3) (17).

$$E_{h\nu}\varphi_i = q_i + \Delta V_i\left(\frac{c_p\rho}{\beta}\right)_T \qquad (3)$$

where q_i is the heat released and ΔV_i is the structural volume change associated with the *i*th process. $E_{h\nu}$ is the excitation molar energy (≡337 kJ/mol at 355 nm), φ_i is the amplitude factor of the acoustic signal associated with the *i*th step, c_p is the specific heat capacity, ρ is the mass density and β is the cubic expansion coefficient of the solvent. In aqueous media, the amplitude of the optoacoustic signal strongly depends on temperature, due to the large temperature variation of β. The $(c_p\rho/\beta)_T$ values were calculated from literature data (18).

Table 1. Decay times, τ_2 (ns), associated with the second component of the LIOAS signals obtained upon excitation of KP^- with 355 nm laser pulses in nonbuffered aqueous solutions, as a function of pH and temperature

Temperature (°C)	pH 6.1	pH 7.5	pH 10.9
9.5			380 ± 20
10			
11	516 ± 20	396 ± 20	
20.9			280 ± 20
21.3			
21.5	357 ± 15	262 ± 10	
28.3			
29.0	280 ± 10	243 ± 10	220 ± 10

As mentioned above, the released heats (intercepts, q_i, of plots such as in Fig. 3) and structural volume changes (slopes, ΔV_i) produced after excitation are separated by using the recovered amplitude factors, φ_i, obtained at different temperatures (*i.e.* different $[c_p\rho/\beta]_T$ values) following (Eq. 3).

The values of q_1 and ΔV_1 are almost pH independent. On the other hand, the q_2 and ΔV_2 values associated with the second LIOAS component are strongly pH dependent (Table 2).

LIOAS measurements in 0.1 *M* phosphate buffer solutions

In order to compare with previous data, LIOAS experiments were also performed with KP^- in 0.1 *M* phosphate buffer solutions. Since the addition of solutes changes the thermoelastic parameters of water, the temperature-dependent $(c_p\rho/\beta)$ ratio for the buffer solutions should be determined. This was carried out by comparing the slopes of the plots of the LIOAS signal amplitudes, *H, vs* the laser total energy for the calorimetric reference in water and in buffer solutions

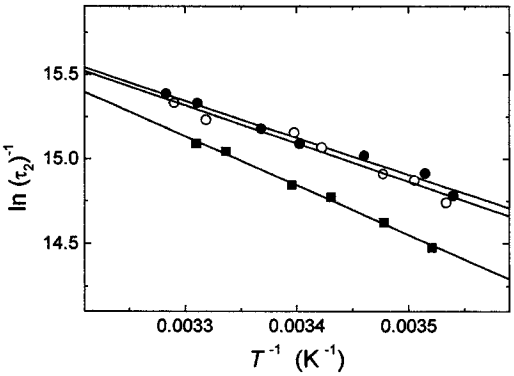

Figure 2. Dependence of the natural logarithm of the inverse of the decay time, τ_2, with the inverse of the temperature in water solutions at (■) pH 6.1 (○) pH 7.5 and (●) pH 10.9.

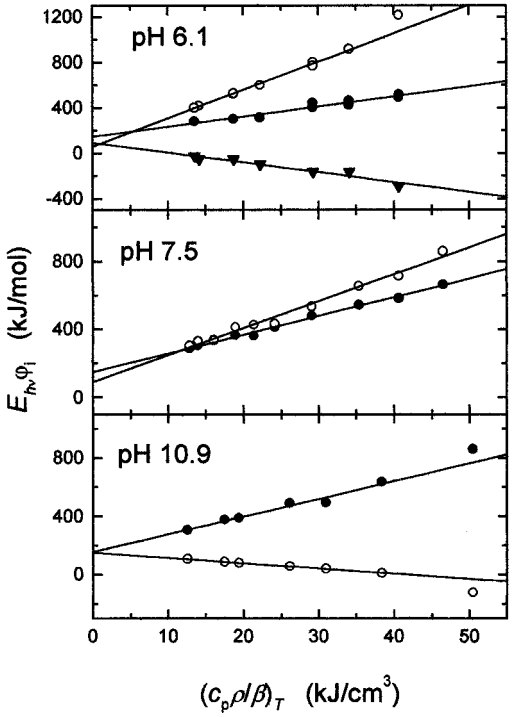

Figure 3. $E_{h\nu}\varphi_i$ values obtained from the analysis of the LIOAS signals of KP^- in buffer-free water at pH 6.1, 7.5 and 10.9 *vs* the ratio $(c_p\rho/\beta)_T$ (temperature range 9.5–31.6°C): (●) $E_{h\nu}\varphi_1$ (first component, τ_1 = 20 ns, fixed); (○) $E_{h\nu}\varphi_2$ (second component, 200 < τ_2 < 550 ns, free); and (▼) $E_{h\nu}\varphi_3$ (third component, τ_3 = 10 μs, fixed).

(Fig. 4) (19). The calculated $(c_p\rho/\beta)_T$ values in buffer solutions were (independent on pH, within the experimental error) (in kJ/cm^3): (31.7 ± 1.5), (27.7 ± 1.3), (23.4 ± 0.8), (21.0 ± 0.9), (17.7 ± 0.8), (16.5 ± 0.7), (15.0 ± 0.5) and (12.9 ± 0.5) at 10, 12, 15, 17, 20, 22, 25 and 30°C, respectively.

The LIOAS signals for KP^- in buffer solutions were also fitted with a sum of exponential decays. As in the case of the buffer-free solutions, three exponential decays were used in the fitting function only at pH 5.7, in order to obtain a satisfactory fit of the signal. The values of q_i and ΔV_i obtained from the linear regression of (Eq. 3) with the φ_i values from the deconvolution analysis and the $(c_p\rho/\beta)_T$ values for the 0.1 *M* buffer solutions are collected in Table 3.

As in the case of the buffer-free water solutions, the values of q_1 and ΔV_1 associated with the ''prompt'' process are pH independent (within experimental error) (Table 3). However, for the second LIOAS component the pH dependence is only observed for q_2. The ΔV_2 values remain almost constant in all the pH range. Note that their values are close to

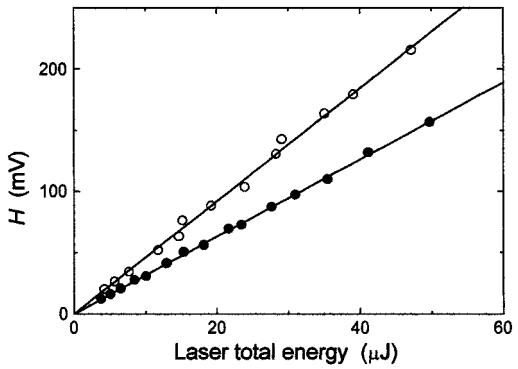

Figure 4. LIOAS signal amplitude *H vs* laser total energy at pH 11 and 10°C for the calorimetric reference Evans blue in: (●) water and (○) in 0.1 *M* phosphate buffer solution.

that observed in the buffer-free solution at pH 10.9, but smaller than those observed at pH 6.1 and 7.5 in the buffer-free solutions.

At a similar temperature (*ca* 25°C), the τ_2 values in buffer solutions are shorter than those in water (Table 3); except for pH *ca* 11, where the decay lifetimes are almost the same within the experimental errors in both media.

DISCUSSION

Under anaerobic conditions KPH photodecarboxylates exclusively from its anion (KP^-, pK_a = 4.7), yielding quantitatively 3-ethylbenzophenone as final product (3,7). The reaction quantum yield is 0.75, constant over the pH range 6.3–12.5 (8). In any case, dissolved CO_2 should be considered a final product in our LIOAS experiments, because the time for the reaction of CO_2 in aqueous medium exceeds by far the upper limit of integration time in our LIOAS experiment, *i.e.* at pH > 10 the reaction $CO_2 + OH^- \rightarrow HCO_3^-$ occurs with a bimolecular rate constant of 6900 M^{-1}/s at 21°C (20), and at pH < 8 the predominant reaction is $CO_2 + H_2O \rightarrow H_2CO_3$, occurring with a pseudo-first order rate constant of 0.03 s^{-1} (21).

''Prompt'' or ''slow'' decarboxylation mechanism

According to our present LIOAS data and the previous laser-flash photolysis studies (8–10), the photodecarboxylation reaction of KP^- should consist of at least two sequential steps. In particular, the decarboxylation step consists of an intramolecular cleavage process involving loss of CO_2 (8–10). Since effective photodecarboxylation of KPH occurs at pH > pK_a = 4.7 (3,7) and with pH-independent quantum yield (8), this step should not be influenced by pH. Therefore, it should be possible to discriminate between the mechanisms

Table 2. Heats released and structural volume changes observed upon excitation of KP^- in nonbuffered aqueous solutions as a function of pH, calculated from deconvolution analysis of the LIOAS signals and evaluation with (Eq. 3) (n.d.: not detected)

pH	q_1 (kJ/mol)	ΔV_1 (mL/mol)	q_2 (kJ/mol)	ΔV_2 (mL/mol)	q_3 (kJ/mol)	ΔV_3 (mL/mol)
6.1	145 ± 20	8.8 ± 0.9	56 ± 20	25.0 ± 1.5	92 ± 30	−8.7 ± 1.0
7.5	146 ± 10	11.0 ± 0.5	89 ± 19	15.0 ± 0.7	n.d.	n.d.
10.9	153 ± 15	12.2 ± 1.0	150 ± 10	−3.6 ± 0.2	n.d.	n.d.

Table 3. Heats released and structural volume changes observed upon excitation of KP^- in 0.1 *M* phosphate buffer solutions as a function of pH, calculated from deconvolution analysis of the LIOAS signals and evaluation with (Eq. 3). Decay times, τ_2 (ns), associated with the second component of the LIOAS signals of KP^- as a function of pH at 25°C are also reported. (n.d: not detected)

pH	q_1 (kJ/mol)	ΔV_1 (cm^3/mol)	q_2 (kJ/mol)	ΔV_2 (cm^3/mol)	τ_2 (ns)	q_3 (kJ/mol)	ΔV_3 (cm^3/mol)
5.7	168 ± 12	7.5 ± 0.5	41 ± 11	−3.3 ± 0.5	136 ± 20	96 ± 30	−5.3 ± 1.5
7.4	170 ± 10	9.3 ± 0.5	91 ± 15	−5.1 ± 0.5	130 ± 15	n.d.	n.d.
11.0	178 ± 15	8.6 ± 0.5	134 ± 10	−3.8 ± 0.5	260 ± 15	n.d.	n.d.

proposed, *i.e.* the ''prompt'' (9,10) or the ''slow'' (8) decarboxylation, by analyzing the pH influence on the heat released and on the sign and magnitude of the structural volume changes for each component of the LIOAS signals.

Our results show that both in water (Table 2) and in 0.1 *M* buffer solutions (Table 3) only the heat and the volume changes associated with the first or ''prompt'' component of the LIOAS signals of KP^- are pH independent. Furthermore, it was reported that the cleavage of an average carbon–carbon bond results in a volume expansion of ~10 cm^3/mol (22). This value is in agreement with our LIOAS measurements for the fast process.

A positive volume change associated with an unimolecular decarboxylation process can also be concluded by a more detailed analysis of the partial molar volume changes contributions involved in the process. In solution, three contributions to the partial molar volume of a solute may be considered: (1) the van der Waals molecular volume V_{vdW}; (2) the contraction of the solvent due to electrostriction effects V_{el} (if electrical charges or permanent dipole moments are created); and (3) a positive contribution resulting from the discontinuous structure of the solvent and the additional void volume in the direct solvent shell surrounding the solvent, V_{ss} (23,24). This latter term results from the perturbation of the packing of the solvent molecules in the liquid due to the addition of a solute molecule (25). In any case, the reaction volume change is the difference between the partial molar volumes of the product(s) and reactant(s): $\Delta V_R = \Delta V_{vdW} + \Delta V_{el} + \Delta V_{ss}$. The latter two contributions have been globally called structural volume changes in our previous studies (14–17,19).

For the decarboxylation step it is expected that the sum of the van der Waals volumes of the products is somewhat larger than that of the reactant species, since bond fragmentation is accompanied by an increase in the molecular surface, so $\Delta V_{vdW} > 0$. Moreover, ΔV_{ss} is also expected to be positive in view of the fact that the perturbation of the liquid structure should increase if the molecular surface of the solutes exposed to the solvent is increased. Immediately after bond break, the fragments of the parent molecule form a contact complex, which subsequently dissociates into free components, with the concomitant increase of the overall volume of the solvent shells surrounding the separated species (24,25).

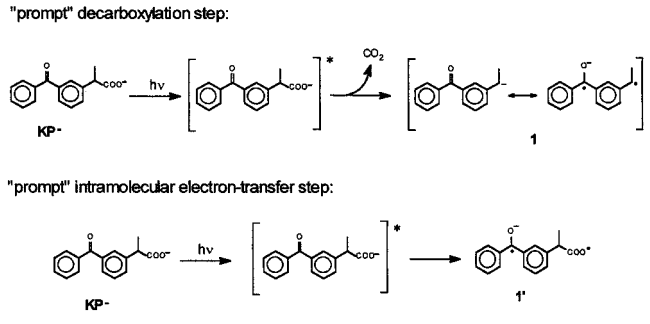

Scheme 1. Reaction scheme representing the ''prompt'' decarboxylation mechanism (top, see Martinez and Scaiano [9]), and the ''slow'' decarboxylation mechanism (bottom, see Monti *et al.* [8]) of KPH carboxylate KP^-.

The sign of the electrostriction contribution, ΔV_{el}, is calculated by using the difference in dipole moment between formed and destroyed species and disregarding specific solute–solvent interactions (26,27). One should now compare the different volume changes occurring during the *fast process*, leading to the formation of the intermediates along the ''prompt'' (9,10) or the ''slow'' (8) decarboxylation mechanisms. In the first case, it was suggested that upon excitation KP^- yields carbanion **1** and CO_2 (Scheme 1).

For the ''slow'' decarboxylation mechanism, the formation of the biradical anion **1′** within *ca* 300 ps after the laser pulse was suggested (Scheme 1) (8).

For the calculations, the reactant is triplet KP^- (see below). The ''prompt'' decarboxylation mechanism (9) predicts an expansion of the van der Waals (VdW) volume on going from $^3KP^-$ to a decarboxylated anion in equilibrium with a biradicaloid form (**1**). From the analysis of the MM+ optimized geometries involved it turns out that the molecular volume of **1** is smaller than that of the precursor KP^- by 3.8 cm^3/mol, a reduction which is largely compensated by the CO_2 loss resulting in an intrinsic global expansion of 29.4 cm^3/mol. On the other hand, the rearrangement of the solvent around the structures involved in the process should give rise to a negative contribution due to the increase in dipole moment ($\Delta\mu$ = 6.9 D), ΔV_{el} = −5.5 cm^3/mol (27), which combined with the intrinsic global expansion of 29.4 cm^3/mol leads to a total positive volume variation of 23.8 cm^3/mol.

For the ''slow'' decarboxylation mechanism (8), we obtain for the fast process (which only implies an electronic rearrangement without CO_2 loss) a global contraction of −14.9 cm^3/mol by taking into account the van der Waals radius of the component atoms and the geometry rearrangement of the biradical **1′**, with a more close-packed molecular shape (radius 3.62 Å) than the more planar initial $^3KP^-$ (radius 4.84 Å). A van der Waals contraction of −39.7 cm^3/mol is in fact only partially compensated by an electrostriction positive contribution ΔV_{el} = +24.8 cm^3/mol due to the dipole moment decrease ($\Delta\mu$ = −13 D). This was calculated

using eq. 3 of Wegewijs *et al.* (14) with the proper μ and r-values but as mentioned above (26,27), disregarding possible solute–solvent specific interactions, which play an important role in water (15,16).

Regarding ΔV_{ss}, we consider that this positive term should be larger for the ''prompt'' scheme, where a fragmentation occurs than for the ''slow'' decarboxylation scheme, where an intramolecular electronic rearrangement takes place. In fact, a calculation of the solvent accessible surface of the intermediates involved in the two mechanisms leads to a reduction from 471 Å^2 for $^3KP^-$ to 440 Å^2 for **1**, which is largely compensated by the release of CO_2, whereas the rearrangement predicted along the passage $^3KP^- \rightarrow \mathbf{1}'$ does not imply any significant difference in such a surface. Therefore, we should consider the calculated reaction volume changes as lower limits of the real values.

In view of the fact that a volume expansion is associated with the fast events (with an average experimental value $\Delta V_1 = [+10.7 \pm 1.7]$ cm^3/mol in water and $\Delta V_1 = [+8.4 \pm 0.6]$ cm^3/mol in 0.1 *M* phosphate buffer solutions, for the pH range studied, Tables 2 and 3), we conclude that a ''prompt'' decarboxylation mechanism in which an expansion is predicted for the fast step is more consistent with the experimental result than the ''slow'' decarboxylation mechanism, which would imply a contraction for the fast electron transfer step.

Photodissociation reactions in solution producing a gas always afford expansions, such as the photolysis of diphenyl-cyclopropenone to diphenylacetylene and CO (23,28–30), and of 1-azidoadamantane to 4-azahomoadamant-3-ene and N_2 (31).

Inasmuch as the decarboxylation step occurs below the time resolution of the LIOAS experiments, we are not able to distinguish if the precursor excited state is a singlet or a short-lived triplet state. Direct evidence of the formation of a subnanosecond triplet state was obtained by using the picosecond laser-flash photolysis (8). However, Cosa *et al.* argue against the role of a triplet state as precursor of the carbanion **1** on the basis of results obtained in basic acetonitrile–water mixtures (10). In any case, intramolecular electron transfer and loss of CO_2 occur both in a time shorter than 10 ns.

pH effect on the transient species

pH plays an important role only for the second LIOAS component (Table 2). The variation of q_2 and ΔV_2 with pH in water solutions indicates that various transient species are formed. Furthermore, different Arrhenius parameters obtained at pH 6.1 and 10.9 (see Fig. 2), support the hypothesis that different transient species are formed at both pH values.

The second species cannot be attributed to the reaction of the detached CO_2 with the solvent, because this reaction occurs in a longer time scale than the upper time resolution of the LIOAS experiment (see above) (20,21). Thus, a reaction of carbanion **1** with the solvent should take place. The preexponential factors obtained for the decay time, τ_2, were around 10^9–10^{10} s^{-1} (Fig. 2). As pointed out by Cosa *et al.* (10) these values may reflect a pseudo-first order reaction, such as the protonation of carbanion **1**, since the Arrhenius parameters are low for a unimolecular bond fragmentation

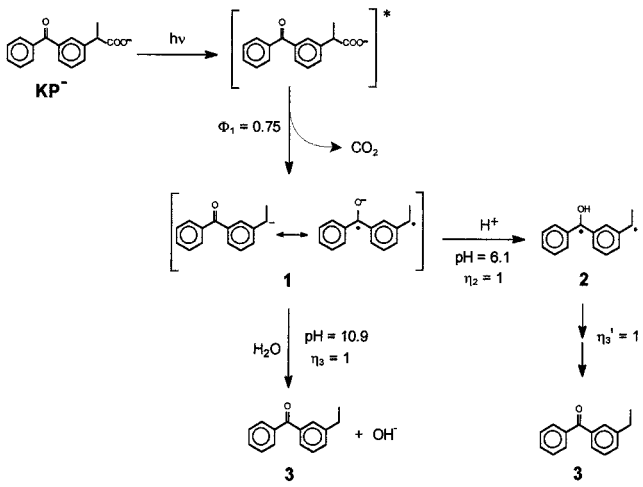

Scheme 2. Reaction scheme for a ''prompt'' decarboxylation process of KPH carboxylate KP^- in water followed by a nanosecond time-scale protonation reaction of carbanion **1** with the media.

(*e.g.* decarboxylation process, with an expected preexponential factor around 10^{13} or higher). These results also support previous conclusions about a ''prompt'' decarboxylation mechanism.

At pH 6.1 a third long-lived component ($\tau_3 \leq 10$ μs) in the LIOAS signal was detected. However, this long-lived component was absent at higher pH, indicating the presence of an intermediate transient species at pH 6.1. Furthermore, the respective q_3 and ΔV_3 values in water solution (Table 2) are similar to those observed in phosphate buffer at pH 5.7 (Table 3). Therefore, the decay of this intermediate does not depend on the composition of the solution.

In view of the analysis presented above and in agreement with previous studies (8–10), we conclude that the mechanism in Scheme 2 accommodates the experimental data available well.

The enthalpy content of the products

Using the ''prompt'' decarboxylation mechanism (Scheme 2), the released heats q_1 and q_2 (Table 2) are used to calculate the enthalpy difference between the intermediate species and ground state KP^-.

In agreement with the model proposed by Martínez and Scaiano (9), the first intermediate should be carbanion **1**, formed upon prompt CO_2 loss and incorporating features of a ketyl radical anion and a benzylic radical. In solution, benzophenone derivatives do not show important energy loss by light emission. Then, the observed prompt heat deposition q_1 (which includes radiationless deactivation and heat released during the intersystem crossing process) is directly related to the enthalpy difference between carbanion **1** and KP^-, ΔH_1, by (Eq. 4),

$$\Delta H_1 = \frac{E_{h\nu} - q_1}{\Phi_1} \qquad (4)$$

where Φ_1 is the quantum yield of the process. In view of the fact that under anaerobic conditions the only final product is 3-ethylbenzophenone, **3**, (3,7) and that the efficiency of $^3KP^-$ formation was estimated as 1 (8), we consider that the quan-

tum yield for the decarboxylation step is 0.75, whereas for the subsequent steps the efficiencies are unity, *i.e.* $\Phi_1 = 0.75$ and $\eta_2 = \eta_3 = \eta_3' = 1$ (see Scheme 2).

Taking into account the pH-independent prompt heat released in water solutions (Table 2), with average value $q_1 = (148 \pm 6)$ kJ/mol (Eq. 4) yields an enthalpy change for the formation of **1**, $\Delta H_1 = (252 \pm 6)$ kJ/mol.

It was reported that carbanion **1** decays directly to **3**, by protonation from the solvent (9). However, we find that transient **1** converts to another (long-lived) transient species in the nanosecond time scale and that the energy difference between both species is pH dependent (q_2, Table 2). Inspection of the q_2 values indicates that an energy-richer transient is formed at pH 6.1 than that at pH 10.9. The q_2 and ΔV_2 values at pH 7.5 are between those at pH 6.1 and 10.9, indicating an intermediate behavior. A protonation equilibrium was postulated between the carbanion **1** and a neutral biradical with ketyl and benzylic centers, **2**, with $pK_a = 7.6$ (8). This biradical **2** is a possible candidate for the intermediate species formed by protonation within 280–500 ns, depending on temperature (Table 1). The enthalpy content of **2** relative to ground state KP^- is thus calculated using (Eq. 5).

$$\Delta H_2 = \frac{E_{h\nu} - (q_1 + q_2)^{pH6.1}}{\Phi_1\eta_2} \quad (5)$$

The term $\Phi_1\eta_2$ is the quantum yield for the formation of **2.** Thus, the enthalpy content of the postulated biradical **2** is $\Delta H_2 = (181 \pm 20)$ kJ/mol, with $\Phi_1\eta_2 = 0.75$, since the formation of **2** occurs sequentially *via* transient **1.**

On the other hand, as the pH increases higher values of q_2 were observed within 200–400 ns after the pulse (Table 1). This result points to the formation of a product with much lower enthalpy content, *i.e.* the direct formation of **3** by protonation from water (8,9). Hence, the enthalpy content of **3** is estimated with (Eq. 6).

$$\Delta H_3 = \frac{E_{h\nu} - (q_1 + q_2)^{pH10.9}}{\Phi_1\eta_3} \quad (6)$$

where $\Phi_1\eta_3 = 0.75$ is the quantum yield for **3** formation at pH 10.9 (Scheme 2). Then, $\Delta H_3 = (45 \pm 15)$ kJ/mol. ΔH_3 is the enthalpy change of the global decarboxylation reaction. Its positive value indicates, as expected, that the total thermal decarboxylation reaction is endothermic.

It was reported that biradical **2** decays to **3** in a multistep process involving times >4 μs (8). In that case, it is also possible to obtain the global enthalpy change ΔH_3 value by using (Eq. 7).

$$\Delta H_3 = \frac{E_{h\nu} - (q_1 + q_2 + q_3)^{pH6.1}}{\Phi_1\eta_2\eta_3'} \quad (7)$$

The term $\Phi_1\eta_2\eta_3' = 0.75$ is the global quantum yield for the formation of **3**, since the formation of the final product at pH 6.1 occurs sequentially *via* transient **1** and **2.** Thus, this calculation yields $\Delta H_3 = (59 \pm 30)$ kJ/mol, in relatively good agreement with the value calculated at pH 10.9 with (Eq. 6). This means that in our LIOAS experimental conditions at pH 6.1, transient **2** decays almost completely to **3** in a time ≤10 μs. However, we note that for this calculation the value of q_3 may be affected by slight differences in baseline between the sample and reference signals (see ''Results''), due to the lower amplitude response of the ceramic transducer in the microsecond time range (11), and the low number of signals averaged (*ca* 10, see the ''Experimental'' section) due to sample depletion. Therefore, we consider that $\Delta H_3 = (45 \pm 15)$ kJ/mol, obtained at pH 10.9, is a more reliable value for the global enthalpy change of the reaction (all values in Table 4).

Table 4. Enthalpy and partial molar volume differences relative to ground state KP^-, $\Delta H_i = (H_i - H_{KP})$ and $\Delta V_i^O = (V_i^O - V_{KP}^O)$, respectively, for the species formed upon excitation of KP^- in aqueous media, interpreted according to the ''prompt'' decarboxylation mechanism, Scheme 2

Species	ΔH_i* (kJ/mol)	ΔH_i† (kJ/mol)	ΔV_i^O* (cm^3/mol)
1	256 ± 10	223 ± 10	−18.9 ± 2.0
2	181 ± 20	173 ± 15	+0.6 ± 2.0
3	45 ± 15	41 ± 15	+14.5 ± 2.0

*Buffer-free water solutions.
†0.1 *M* phosphate buffer solutions.

The partial molar volumes of the products

Quantitative interpretation of structural volume changes in aqueous media is a complicated issue, in view of the possible specific interactions and/or to electrostriction effects changing upon reaction (24,26,32).

Following Scheme 2, the ''prompt'' step involves the formation of carbanion **1** and CO_2 with a quantum yield $\Phi_1 = 0.75$. With the value of ΔV_1 and the respective quantum yield, the molar structural volume change per photoconverted mol (Eq. 8), $\Delta V_{R,1}$ is calculated (17).

$$\Delta V_{R,1} = \frac{\Delta V_1}{\Phi_1} \quad (8)$$

As was mentioned, the ''prompt'' process is pH independent. Therefore, by using (Eq. 7) with the average value $\Delta V_1 = (+10.7 \pm 0.6)$ cm^3/mol (Table 2), a value $\Delta V_{R,1} = (+14.3 \pm 0.6)$ cm^3/mol is obtained. This volume change represents the difference between the partial molar volumes of the products (carbanion **1** and CO_2) and that of KP^- (Eq. 9).

$$\Delta V_{R,1} = (V_{CO_2}^O + V_1^O) - V_{KP^-}^O \quad (9)$$

By rearranging (Eq. 9), the partial molar volume difference between carbanion **1** and KP^- is calculated to be $\Delta V_1^O = (V_1^O - V_{KP^-}^O) = (-18.9 \pm 2)$ cm^3/mol, with $V_{CO_2}^O = 33.2$ cm^3/mol in water (33). The drastic partial molar volume reduction of species **1** with respect to KP^- is an obvious consequence of the CO_2 loss.

At pH 6.1, a large expansion is observed upon decay of **1** to the neutral biradical **2.** This process involves a charge neutralization reaction between the carbanion **1** and H^+, producing a decrease in electrostriction due to the lack of electrical charges (Scheme 2). However, additional effects due to specific solvent interactions, such as hydrogen bonding, cannot be ruled out. The larger Arrhenius preexponential factor at pH 6.1 should reflect an entropic gain associated with the large volume expansion observed at this pH. Since the process $\mathbf{1} + H^+ \rightarrow \mathbf{2}$ occurs with $\eta_2 = 1$, the ΔV_2 value

is directly the reaction volume change per phototransformed species, $\Delta V_{R,2}$, which represents the following balance of partial molar volumes (Eq. 10).

$$\Delta V_{R,2}^{pH\ 6.1} = V_2^O - (V_1^O + V_{H^+}^O) \quad (10)$$

where $V_{H^+}^O = -5.5$ cm^3/mol is the partial molar volume of the H^+ in water (34). The partial molar volume difference between **2** and KP^-, $\Delta V_2^O = (V_2^O - V_{KP^-}^O) = (+0.6 \pm 2)$ cm^3/mol is obtained by replacing $\Delta V_1^O = (V_1^O - V_{KP^-}^O)$ in (Eq. 10).

The partial molar volume difference between **3** and KP^- is obtained from the ΔV_2 value at pH 10.9. Following Scheme 2, transient **1** decays to **3**, upon reaction with the solvent, **1** + $H_2O \rightarrow$ **3** + OH^-. Since the efficiency of the process $\eta_3 = 1$, the ΔV_2 value is directly the reaction volume change per phototransformed species, $\Delta V_{R,2}$. Therefore, the balance of partial molar volumes is given by (Eq. 11).

$$\Delta V_{R,2}^{pH\ 10.9} = (V_3^O + V_{OH^-}^O) - (V_1^O + V_{H_2O}^O) \quad (11)$$

where $V_{OH^-}^O = -12.5$ cm^3/mol (32) and $V_{H_2O}^O = 24.5$ cm^3/mol (35) are the partial molar volume of the hydroxide ion and water at room temperature, respectively. Again, by using the ΔV_1^O value, the partial molar volume difference between **3** and KP^-, $\Delta V_3^O = (V_3^O - V_{KP^-}^O) = (+14.5 \pm 2)$ cm^3/mol is obtained. All the calculated partial molar volume differences are collected in Table 4.

It was recently reported that in the keto-enol photoconversion of 2-methylbenzophenone, the molecular volume is reduced about 12 cm^3/mol by transformation from the keto to the enol forms due to intermolecular hydrogen bonding with the solvent (36). Hydrogen bonding plays an important role in the magnitude and sign of structural volume changes with solutes containing groups with Lewis acid–base properties, such as in the case of some inorganic complexes (15,16,34) and organic dyes (37). The partial molar volume difference between the species **3** and **2** is almost the same as that observed by Terazima for the photoenolization of 2-methylbenzophenone (36), indicating that the hydrogen bonding interactions with the solvent are larger for **2** than for **3**.

Note that in spite of the CO_2 loss, the neutral species **2** and **3** have larger partial molar volume than ground state KP^-. This is an indication of the important role played by the electrical charge located at the carboxylate group of KP^-, which increases the electrostriction effect upon the solvation shell.

Buffer effect on the structural volume changes

In contrast to the behavior in buffer-free solution, in 0.1 *M* phosphate buffer solutions the ΔV_2 values (around -4 cm^3/mol) are almost pH independent (Table 3). This effect is explained by considering that at low pH (*e.g.* pH 6.1) carbanion **1** reacts with species constituting the buffer, such as $H_2PO_4^-$, present in high concentration (Eq. 12).

$$H_2PO_4^- + \mathbf{1} \rightarrow HPO_4^{2-} + \mathbf{2} \quad (12)$$

Kurian and Small (38) reported that the structural volume changes occurring in proton-transfer reactions are strongly affected by the nature of the buffer species present. In particular, at pH 7 the reaction $H_2PO_4^- \rightarrow HPO_4^{2-} + H^+$ is accompanied by a volume contraction of -26 cm^3/mol (39), due to the increment of the electrical charges. In our case, the large expansion observed for the decay of **1** to **2** at low pH values should be compensated by the volume contraction produced by the change on the speciation of the buffer ionic species. Instead, at higher pH values, *i.e.* at pH 11, this effect is not observed since **1** reacts with solvent molecules (see above) and the structural volume change ΔV_2 is the same as that observed in buffer-free solutions.

The concept of **1** reacting with buffer species is also supported by the shorter decay time observed in these media than in buffer-free media, in particular at low pH (compare Tables 2 and 3).

In contrast to the structural volume changes that are strongly affected by the presence of phosphate buffer; the differences in the heat released with and without buffer are smaller. In fact, by using (Eqs. 4–6) with the q_1 and q_2 values in buffer media, similar enthalpy contents for species **2** and **3** were calculated, as for the buffer-free media (Table 4). For species **1** the difference is somehow larger. The relatively small difference for the enthalpy changes between buffered and unbuffered solutions are in line with the small changes reported in the literature for the heat of proton ionization of organic acids as a function of ionic strength (see, *e.g.* the values for benzoic acid *vs.* ionic strength) (40). Thus, the major perturbation introduced by the buffer is of entropic nature, *i.e.* the solvent rearrangement induced by the reaction of the intermediates with the ionic species in the buffer.

CONCLUSIONS

In summary, LIOAS yields valuable information for the elucidation of the KPH photodecarboxylation mechanism. Under anaerobic conditions, the first step is the formation of carbanion **1** and CO_2 loss within the nanosecond laser pulse. Our present LIOAS data is thus in agreement with the suggestion (9) based on the analysis of the Arrhenius parameters for the decay of **1**, that the latter species cannot suffer decarboxylation but rather, fast decarboxylation takes place within the nanosecond laser pulse (10).

Subsequently, the decay of **1** in the nanosecond time-scale is clearly pH-dependent due to the formation of a long-lived species (probably biradical **2**) at pH $<$ 7.6, or to the direct formation of the final product **3** at pH $>$ 7.6, as proposed (8). Biradical **2** is produced by protonation of **1** from the solvent or by proton-transfer reaction from a buffer species (if such type of species is present). In turn, biradical **2** decays to **3** within $<$10 μs. Instead, at pH $>$ 7.6, the direct formation of **3** is produced by reaction with H_2O in the nanosecond time-scale, since no buffer effect was observed at high pH values.

The presence of phosphate buffer mainly affects the structural volume changes observed, due to the change in the speciation of the ionic buffer species after the proton-transfer reaction. In turn, the change of speciation alters the electrostriction balance in the solution. Thus, in general, data obtained in buffer media (especially structural volume changes) must be carefully interpreted.

Acknowledgements—C.D.B. thanks the Consejo Nacional de Investigaciones Científicas y Técnicas (CONICET, Argentina) and the Agencia Nacional de Promoción Científica y Tecnológica de la Ar-

gentina (Project PICT98 #06–3770), and S.S. thanks ''MURST: Cofinanziamento di Programmi di Rilevante Interesse Nazionale'' for financial support. We thank Dagmar Lenk for her able technical assistance and Prof. Kurt Schaffner for his constant support.

REFERENCES

1. Budac, D. and P. Wan (1992) Photodecarboxylation mechanism and synthetic utility. *J. Photochem. Photobiol. A: Chem.* **67**, 135–166.
2. Boscá, F. and M. A. Miranda (1998) Photosensitizing drugs containing the benzophenone chromophore. *J. Photochem. Photobiol. B: Biol.* **43**, 1–26.
3. Costanzo, L. L., G. De Guidi, G. Condorelli, A. Cambria and M. Fama (1989) Molecular mechanism of drug photosensitization. II. Photohemolysis sensitized by ketoprofen. *Photochem. Photobiol.* **50**, 359–365.
4. Artuso, T., J. Bernadou, B. Meunier, J. Piette and N. Paillous (1991) Mechanism of DNA cleavage mediated by photoexcited non-steroidal antiinflammatory drugs. *Photochem. Photobiol.* **54**, 205–213.
5. Marguery, M. C., N. Chouini-Lalanne, J. C. Ader and N. Paillous (1998) Comparison of the DNA damage photoinduced by fenofibrate and ketoprofen, two phototoxic drugs of parent structure. *Photochem. Photobiol.* **68**, 679–684.
6. Chignell, C. F. and R. H. Silk (1998) The effect of static magnetic fields on the photohemolysis of human erythrocytes by ketoprofen. *Photochem. Photobiol.* **67**, 591–595.
7. Boscá, F., M. A. Miranda, G. Carganico and D. Mauleón (1994) Photochemical and photobiological properties of ketoprofen associated with the benzophenone chromophore. *Photochem. Photobiol.* **60**, 96–101.
8. Monti, S., S. Sortino, G. De Guidi and G. Marconi (1997) Photochemistry of 2-(3-benzoylphenyl)propionic acid (ketoprofen). Part 1. A picosecond and nanosecond time resolved study in aqueous solution. *J. Chem. Soc., Faraday Trans.* **93**, 2269–2275.
9. Martínez, L. J. and J. C. Scaiano (1997) Transient intermediates in the laser flash photolysis of ketoprofen in aqueous solutions: unusual photochemistry for the benzophenone chromophore. *J. Am. Chem. Soc.* **119**, 11 066–11 070.
10. Cosa, G., L. Martínez, L. and J. C. Scaiano (1999) Influence of solvent polarity and base concentration on the photochemistry of ketoprofen: independent singlet and triplet pathways. *Phys. Chem. Chem. Phys.* **1**, 3533–3537.
11. Rudzki, J. E., J. L. Goodman and K. S. Peters (1985) Simultaneous determination of photoreaction dynamics and energetics using pulsed, time-resolved photoacoustic calorimetry. *J. Am. Chem. Soc.* **107**, 7849–7854.
12. Perrot, G., B. Cheng, K. D. Gibson, J. Vila, K. A. Palmer, A. Nayeem, B. Maigret and H. A. Sheraga (1992) A program for the rapid analytical determination of accessible surface areas and their derivatives. *J. Comput. Chem.* **13**, 1–11.
13. Mataga, N. and T. Kubota (1970) *Molecular Interactions and Electronic Spectra*, Chap. 8. Marcel Dekker, New York.
14. Wegewijs, B., J. W. Verhoeven and S. E. Braslavsky (1996) Volume changes associated with intramolecular exciplex formation in a semiflexible donor-bridge-acceptor compound. *J. Phys. Chem.* **100**, 8890–8894.
15. Borsarelli, C. D. and S. E. Braslavsky (1998) Volume changes correlate with enthalpy changes during the photoinduced formation of the MLCT state of ruthenium(II) bipyridine cyano complexes in the presence of salts. A case of entropy—enthalpy compensation effect. *J. Phys. Chem. B* **102**, 6231–6238.
16. Borsarelli, C. D. and S. E. Braslavsky (1999) Enthalpy, volume, and entropy changes associated with the electron transfer reaction between the ^{3}MLCT state of $Ru(bpy)_3^{2+}$ and methyl viologen cation in aqueous solutions. *J. Phys. Chem. A* **103**, 1719–1727.
17. Braslavsky, S. E. and G. E. Heibel (1992) Time-resolved photothermal and photoacoustic methods applied to photoinduced processes in solution. *Chem. Rev.* **92**, 1381–1410.
18. Weast, R. C. (Ed.)(1986–1987) *CRC Handbook of Chemistry and Physics*, 67th Ed., pp. F-4, F-5. CRC Press, Boca Raton.
19. Churio, M. S., K. P. Angermund and S. E. Braslavsky (1994) Combination of laser-induced optoacoustic spectroscopy (LIOAS) and semiempirical calculations for the determination of molecular volume changes. The photoisomerization of carbocyanines. *J. Phys. Chem.* **98**, 1776–1782.
20. Schuchmann, M. N. and C. von Sonntag (1982) Determination of the rate constants of the reactions $CO_2 + OH^- \rightarrow HCO_3$ and barbituric acid $\rightarrow$ barbiturate anion + H^+ using pulse-radiolysis technique. *Z. Naturforsch. B* **37**, 1184–1186.
21. Cotton, F. A. and G. Wilkinson (1966) *Advanced Inorganic Chemistry*. Wiley, New York.
22. Le Noble, W. J. and H. Kelm (1980) Chemistry in compressed solutions. *Angew. Chem., Int. Ed. Engl.* **19**, 841–856.
23. Schmidt, R. and M. Schütz (1996) Determination of reaction volumes and reaction enthalpies by photoacoustic calorimetry. *Chem. Phys. Lett.* **263**, 795–802.
24. Schmidt, R. (1998) Interpretation of reaction and activation volumes in solution. *J. Phys. Chem A* **102**, 9082–9086.
25. Yoshimura, Y. and M. Nakahara (1984) Molecular theory of the volume change accompanying contact-complex formation reactions in solution. *J. Chem. Phys.* **81**, 4080–4086.
26. Whalley, E. (1963) Some comments on electrostatic volumes and entropies of solvation. *J. Chem. Phys.* **38**, 1400–1405.
27. $\Delta V_{el} = -(\mu^2/r^3)\,[(\epsilon + 2)\,(\epsilon - 1)]/(2\epsilon + 1)2\,\kappa T$
28. Herman, M. S. and J. L. Goodman (1989) Determination of the enthalpy and reaction volume changes of organic photoreactions using photoacoustic calorimetry. *J. Am. Chem. Soc.* **111**, 1849–1854.
29. Hung, R. R. and J. J. Graboswski (1992) Enthalpy measurements in organic solvents by photoacoustic calorimetry: a solution to the reaction volume problem. *J. Am. Chem. Soc.* **114**, 351–353.
30. Terazima, M., T. Hara and N. Hirota (1995) Reaction volume and enthalpy changes in photochemical reaction detected by the transient grating method; photodissociation of diphenylcyclopropenone. *Chem. Phys. Lett.* **246**, 577–582.
31. Wayne, G. S. and G. J. Snyder (1993) Measurement of the strain energy of a transient bridgehead imine, 4-azahomoadamat-3-ene, by photoacoustic calorimetry. *J. Am. Chem. Soc.* **115**, 9860–9861.
32. Millero, F. (1971) The molal volumes of electrolytes. *Chem. Rev.* **71**, 147–176.
33. Malinin, S. D. (1974) Questions concerning thermodynamics of H_2O_2–CO_2 system. *Geokhimiya* **10**, 1523–1549.
34. Borsarelli, C. D. and S. E. Braslavsky (1998) The partial molar volume of the proton in water determined by laser-induced optoacoustic studies. *J. Photochem. Photobiol. B: Biol.* **43**, 222–228.
35. Bonetti, G., A. Vecli and C. Viappiani (1997) Reaction volume of water detected by time-resolved photoacoustics: photoinduced proton transfer between *o*-nitrobezaldehyde and hydroxyls in water. *Chem. Phys. Lett.* **269**, 268–273.
36. Terazima, M. (1998) Reaction enthalpy and reaction volume changes upon photoenolization: 2-methylbenzophenone. *J. Phys. Chem. A* **102**, 545–551.
37. Gensch, T. and S. E. Braslavsky (1997) Volume changes related to triplet formation of water-soluble porphyrins. A laser-induced optoacoustic spectroscopy (LIOAS) study. *J. Phys. Chem. B* **101**, 101–108.
38. Kurian, E. and J. R. Small (1995) Volumetric photoacoustic spectroscopy. Listening to more than just heat. *Spectroscopy* **10**, 27–33.
39. Van Eldik, R., T. Asano and W. J. Le Noble (1989) Activation and reaction volumes in solutions. 2. *Chem. Rev.* **89**, 549–688.
40. Izatt, R. M. and J. J. Christensen (1970) *CRC Handbook of Biochemistry*, 2nd Ed. (Edited by H. A. Sober), p. J-83. The Chemical Rubber Co., Cleveland.